Network synchronization in hippocampal neurons

Yaron Penn[a], Menahem Segal[b], and Elisha Moses[a,1]

[a]Department of Physics of Complex Systems, The Weizmann Institute of Science, Rehovot 76100, Israel; and [b]Department of Neurobiology, The Weizmann Institute of Science, Rehovot 76100, Israel

Edited by Michael Hasselmo, Boston University, Boston, MA, and accepted by the Editorial Board January 27, 2016 (received for review July 30, 2015)

Oscillatory activity is widespread in dynamic neuronal networks. The main paradigm for the origin of periodicity consists of specialized pacemaking elements that synchronize and drive the rest of the network; however, other models exist. Here, we studied the spontaneous emergence of synchronized periodic bursting in a network of cultured dissociated neurons from rat hippocampus and cortex. Surprisingly, about 60% of all active neurons were self-sustained oscillators when disconnected, each with its own natural frequency. The individual neuron's tendency to oscillate and the corresponding oscillation frequency are controlled by its excitability. The single neuron intrinsic oscillations were blocked by riluzole, and are thus dependent on persistent sodium leak currents. Upon a gradual retrieval of connectivity, the synchrony evolves: Loose synchrony appears already at weak connectivity, with the oscillators converging to one common oscillation frequency, yet shifted in phase across the population. Further strengthening of the connectivity causes a reduction in the mean phase shifts until zero-lag is achieved, manifested by synchronous periodic network bursts. Interestingly, the frequency of network bursting matches the average of the intrinsic frequencies. Overall, the network behaves like other universal systems, where order emerges spontaneously by entrainment of independent rhythmic units. Although simplified with respect to circuitry in the brain, our results attribute a basic functional role for intrinsic single neuron excitability mechanisms in driving the network's activity and dynamics, contributing to our understanding of developing neural circuits.

neuron | network | oscillator | synchrony | persistent Na current

Periodicity emerges as a key physiological characteristic at all levels of neuronal activity, from the dynamics of neurons at subthreshold potentials (1, 2), through rhythmic neuronal ensembles within local networks, and all of the way up to global oscillations measured by electroencephalography (EEG) (3). The range of observed frequencies is surprisingly wide, from the millisecond range typical for interspike intervals all of the way to several seconds in the case of slow EEG. Over the years, accumulating evidence and theory have attributed different mechanisms for the origin of each measured periodic activity. Within local networks, the role of known collective mechanisms for periodicity, such as the balance between excitatory and inhibitory neurons and recurrent network architecture (4–6), is often contrasted with single neuron contributions, for example, the role of pacemaker neurons in oscillatory network dynamics (7). Although the physiological properties of single neurons are diverse and well documented (2, 8), their role in emergent network oscillations was predicted theoretically (9), but has not been observed experimentally. This contribution may involve a subtle interplay between intrinsic excitability and network connectivity (10, 11).

The connectivity and excitability together determine the behavior of the network. The connectivity can be decreased either at the receiving, postsynaptic neuron or at the sending, presynaptic neuron. The postsynaptic end is blocked by the use of appropriate synaptic blockers. The presynaptic end can be modified by decreasing $[Ca^{2+}]_o$ in the environment and effectively stopping synaptic vesicle release.

To understand excitability, one must take into account the origin of membrane potential fluctuations, which can drive a single neuron to fire action potentials (APs). Although APs of coupled neurons are usually triggered via an "integrate and fire" process, there is also evidence for synapse-independent intrinsic processes capable of driving APs (11). Both synaptic and intrinsic processes affect the excitability state of the cell, which, in turn, determines how close to threshold the cell hovers before firing.

The excitability can also be modulated by the balance between intracellular and extracellular ionic concentrations. Changes in the extracellular ionic environment can be globally controlled and take effect immediately without relying on adaptive mechanisms. The effect of changes in the ionic environment on intrinsic excitability can be striking (7, 12). The potassium concentration directly affects the resting membrane potential of the neuron, but other subtle effects can also arise from divalent ions that affect specific channel activity, and thus the internal excitability of the cell.

In particular, calcium plays an important role in controlling collective behavior by participating in synaptic transmission between neurons, regulating the release of neurotransmitter vesicles (13). Furthermore, calcium is important for determining the single cell excitability, for example, by regulating leak currents into the neuron via the NALCN (sodium leak channel) (14, 15).

In this study, we modified both excitability and connectivity by systematically varying the network environment, and we used multielectrode arrays (MEAs) to follow the spontaneous activity of up to 59 single neurons continuously and simultaneously in a dissociated culture. The large-scale network bursting that is characteristic of dissociated culture activity is easily monitored with single spike resolution in this system (16). The precise control of external conditions, along with a high temporal resolution and the relatively large number of recorded neurons in this system, makes it possible to search for the role of heterogeneous intrinsic properties of single neurons in the emergence of synchronized network bursts.

Results

The characteristic behavior of mature [14–17 d in vitro (DIV)] neuronal cultures in standard physiological medium (1–1.5 mM

Significance

We show that neurons from the hippocampus and cortex fire in an oscillatory manner, both individually and as a network. When disconnected, the majority of neurons are independent intrinsic oscillators, each with its own natural frequency. Synchronization of the neurons occurs when coupling is introduced. Weak coupling already leads to convergence of all of the oscillators to one common oscillation frequency. Strikingly, this common frequency is close to the mean distribution of their natural frequencies. Strengthening the coupling decreases the phase differences of the oscillators to practically zero, leading to synchronous periodic network bursts. Overall, we show that periodic network bursts originate in collective effects rather than in specialized pacemaking elements that control the rest of the network.

Author contributions: Y.P., M.S., and E.M. designed research; Y.P., M.S., and E.M. performed research; Y.P. analyzed data; and Y.P. and E.M. wrote the paper.

The authors declare no conflict of interest.

This article is a PNAS Direct Submission. M.H. is a guest editor invited by the Editorial Board.

[1]To whom correspondence should be addressed. Email: elisha.moses@weizmann.ac.il.

This article contains supporting information online at www.pnas.org/lookup/suppl/doi:10.1073/pnas.1515105113/-/DCSupplemental.

$[Ca^{2+}]_o$, 1 mM $[Mg^{2+}]_o$, and 4–5 mM $[K^+]_o$) consisted of periodic bursting. As seen in Fig. 1 *A* and *B*, these periodic bursts were highly synchronized network bursts in which activity typically lasted up to several seconds. The activity was separated by windows of complete silence, which may vary in duration depending on the ionic composition of the medium.

The stability of the periodic bursts was demonstrated by using the three different measurement techniques of MEAs, patch-clamp electrophysiology, and fluorescent imaging in parallel (data are shown in Figs. S1–S4). Fast Fourier analysis of the bursting behavior in the MEAs showed a stable bursting amplitude and frequency for as long as the measurement continued (over 2 h; Fig. S1). Analysis of the interburst intervals (IBIs), or quiet time between bursts, showed peaked distributions for all three measurement modalities in more than 20 cultures measured. The coefficient of variation (CV) of the IBI distribution was typically CV ~ 0.4, which is indicative of well-defined oscillation frequencies (MEA, fluorescence, and patch-clamp measurements are shown in Figs. S2–S4, respectively). Each neuron fired, on average, 7.6 ± 1.0 (mean ± SEM) spikes per burst (n = 8 cultures, total number of electrodes = 259). The bursting network activity involved the participation of all of the recorded neurons, with a typical recruitment time (as defined in *SI Materials and Methods*, *Analysis*) of 30–40 ms.

In contrast, we found that varying the medium to include undefined components by addition of horse serum immediately changes the culture's behavior to a less stable, more complex repertoire of dynamics with no obvious periodicity (Fig. S5). Reverting back to medium with no horse serum results in immediate recovery to the stable oscillatory state. In both cases, the change is abrupt with little apparent adaptation.

Upon removal of the extracellular calcium (0 mM $[Ca^{2+}]_o$), we found that over 85% of the single neurons maintained their firing with only a small reduction in the mean firing rate (Fig. 1*I*). However, the drastic and immediate change was in the complete abolishment of collective behavior, as shown in Fig. 1 *C*, *D*, and *J*. The loss of connectivity within the population led to the disappearance of network bursts, whereas activity persisted in over 85% of the single neurons (Fig. 1 *C* and *D*). Controlling for the existence of residual calcium in the medium with the calcium chelator EGTA (1 mM) showed no change in the behavior (Fig. S6).

The calcium-free medium is known to affect the connectivity in the network by reducing presynaptic vesicle release (17, 18). For comparison, we also blocked the postsynaptic end by addition of saturating concentrations of the synaptic blockers 6-cyano-7-nitroquinoxaline-2,3-dione; 2-amino-5 phosphonovaleric acid; and bicuculline, completely abolishing synaptic transmission. Fig. 1 *E*–*H* shows its effect on both network bursting (at 1 mM $[Ca^{2+}]_o$) and single neuron activity (at 0 mM $[Ca^{2+}]_o$). In the calcium-free case, there was little to no effect of the additional blocking (Fig. 1 *G* and *H*), indicating that the activity recorded under calcium-free conditions was intrinsic and already independent of synaptic communication. Surprisingly, the synaptic blockers caused the cessation of all activity in the standard calcium-containing medium (Fig. 1*I*). Although this drastic disruption of activity by blockers has been reported previously, its origin was unknown. Fig. 1 *E* and *F* shows an intermediate effect of synaptic blockers under the condition of 1 mM $[Ca^{2+}]_o$, where some single neuron activity persisted but the network bursts disappeared.

A fundamental question is therefore why single neuron activity persists when synaptic connectivity is disrupted by eliminating vesicle release, but ceases when it is disrupted by blocking receptors. The fact that the single neuron activity is reduced when the concentration of $[Ca^{2+}]_o$ is increased suggests the involvement of neuronal excitability in determining the intrinsic neuronal firing. Indeed, holding the $[Ca^{2+}]_o$ level at 1.5 mM while increasing the potassium level to 7 mM, equivalent to about 6 mV of depolarization of the membrane resting potential, led 40% of the active neurons to resume the intrinsic activity even with synaptic blockers, at a level

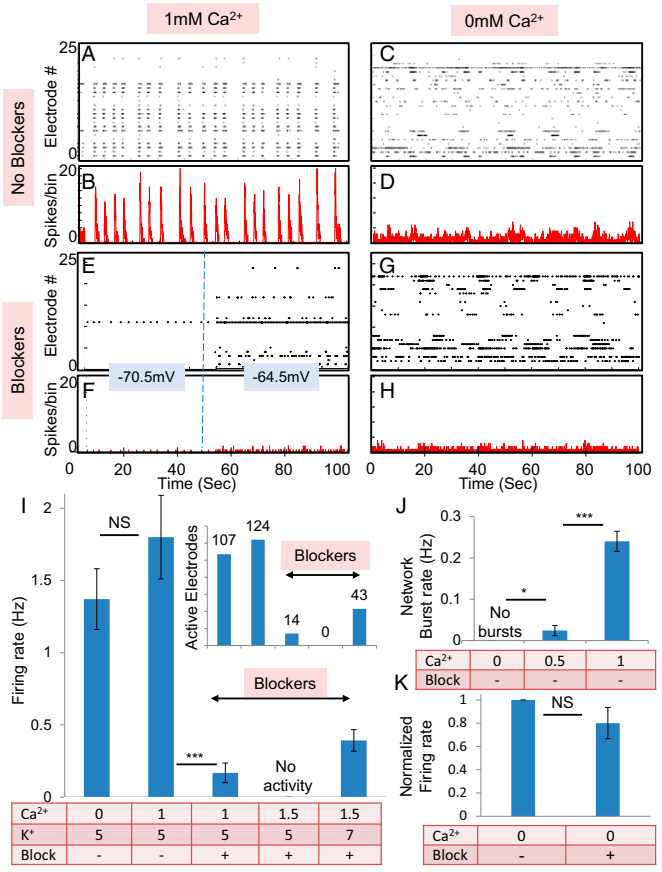

Fig. 1. Bursting network activity at 1 mM Ca^{2+} vs. independent, asynchronous intrinsic neuronal activity at 0 mM Ca^{2+}. Typical raster plots (*A*) and integrated network firing rates (*B*, red) of MEA electrodes (n = 25) at 1 mM Ca^{2+} show periodic bursting behavior. (*C* and *D*) Same culture at 0 mM Ca^{2+} exhibits asynchronous firing with no bursts, whereas the single neurons maintain their firing rate (statistics in *I*). (*E* and *F*) Application of synaptic blocks at 1 mM Ca^{2+} abolishes practically all activity, whereas depolarization using 7 mM K^+ instead of 4 mM K^+ recuperates a considerable fraction of the activity, which is asynchronous and not bursting (statistics in *I*). (*G* and *H*) At 0 mM Ca^{2+}, the same synaptic blockade has practically no effect on the firing pattern (statistics in *K*). Network firing rates reported in *B*, *D*, *F*, and *H* are the total number of spikes measured over all of the active electrodes in 20-ms bins. In contrast, the single neuron firing rate given in *I* and *K* is calculated by dividing the total number of spikes that a single neuron fired in a given experimental condition by the duration of the measurement, and then averaging over neurons. The burst rate reported in *J* is the number of network bursts detected (criteria in *Materials and Methods* and *SI Materials and Methods*, *Analysis*) divided by the duration. Membrane potentials (–70.5 mV and –64.5 mV) in *F* were obtained from the Goldman–Hodgkins–Katz equation for 4 mM K^+ and 7 mM K^+, respectively. (*I*) Summary of statistics for firing rates at different Ca^{2+} and K^+ concentrations, with and without synaptic blockers (*P < 0.05; ***P < 0.001). (*Inset*) Number of active electrodes under the same conditions. (*J*) Synchronous network bursts appear at 1 mM Ca^{2+}. At 0.5 mM Ca^{2+}, some cultures already exhibited zero-lag synchronous bursting, but most did not, creating an intermediate state (***P < 0.001). (*K*) Comparison of average single neuron firing rate at 0 mM Ca^{2+} before and after application of synaptic blockers (normalized by the maximal single neuron firing rate in the culture). No significant change is apparent (t test: P = 0.197; NS, not significant).

of about one-third of the firing rate at 0 mM $[Ca^{2+}]_o$ (Fig. 1 *E*, *F*, and *I*). As expected, however, the synchronized network bursting activity did not recover. Decreasing the excitability by addition of 3 mM Mg^{2+} (19) had the opposite effect of reducing the intrinsic single neuron activity either with or without synaptic blockers, and for both 0 mM $[Ca^{2+}]_o$ and 1.5 mM $[Ca^{2+}]_o$ (Fig. S7).

The Majority of Dissociated Neurons Are Self-Sustaining Oscillators. Inspection of the intrinsic firing pattern of single neurons during the asynchronous activity at 0 mM $[Ca^{2+}]_o$ revealed that about two-thirds of the neurons were, in fact, oscillators (Fig. 2). Because about 85% of all of the active neurons continue to fire at 0 mM $[Ca^{2+}]_o$, in total about 2/3 of 0.85, or ~60% of all active neurons are oscillators. The oscillating neurons fired a number of spikes once per cycle and were quiescent during the rest of the cycle. As seen in Fig. 2 *A*–*C*, both the fast Fourier transform (FFT) power spectrum and the autocorrelation function show a clear signature of the dominant frequency. The remaining 30–40% of the neurons did not show a clear periodic signature (*Materials and Methods* and *SI Materials and Methods*, *Analysis*).

The distribution of oscillation frequencies for the different neurons within the same culture was rather broad, and could range from 0.05 to 0.8 Hz (Fig. 2*D*), with a few outliers (3 of 277) that oscillate at up to 1.5 Hz. These frequencies were stable for as long as we monitored them, and the distribution of IBIs had a CV of ~0.3 (Fig. S8). Although most of the experiments were performed with hippocampal neurons, we verified that cortical cultures exhibit similar oscillatory behavior. The fraction of oscillatory neurons in cortical and hippocampal cultures was the same, but the frequencies were shifted to higher values in cortical neurons (Fig. 2*D*).

The effect of changes in excitability was assessed by steps of increased potassium concentration so as to control membrane potential. As shown in Fig. 2*D*, the distribution of frequencies at 7 mM $[K^+]_o$ was similar but slightly shifted to higher frequencies compared with 5 mM $[K^+]_o$. A more detailed dependence is shown in Fig. 2 *E* and *F*, where the increase in average frequency is seen to be threefold over the range of 1–7 mM $[K^+]_o$. The firing rate also increased proportionally (Fig. 2*E*), whereas the number of spikes per burst did not change significantly (Fig. 2*F*). Taken together, as excitability was increased by increased $[K^+]_o$ levels, the neurons decreased the time of quiescence between bursts with little change in the burst spike composition.

Synchrony Emerges as a Transition from Independently Oscillating Single Neurons into Coherent Network Bursts. The coupling of intrinsic oscillators and the subsequent emergence of network dynamics are of conceptual interest and have been systematically treated theoretically (20, 21). Following the finding of intrinsic oscillators (Fig. 2), we further explored the issue of coupling. As the calcium concentration was gradually increased from 0 to 500 μM (Fig. 3*A*), thus enabling connectivity, a transition from an ensemble of individually firing oscillators to a coherent synchronized network of bursts was evident (the transition is displayed in Movies S1–S4). One hundred micromolar $[Ca^{2+}]_o$ was sufficient to coordinate the neuronal activity along a slow time scale measured in seconds. Although no network bursts emerged at this concentration, the neurons had already adjusted their activity to one common oscillation frequency, shifted in phase across the population. Phase-shift adjustment of the neuron oscillations to zero-lag gradually developed with increased $[Ca^{2+}]_o$ until the activity was fully synchronized at 500 μM.

The gradual synchronization was well captured by the cross-correlation among the activities of all individual neurons (Fig. 3*C*). Although the phases were widely distributed at 100 and 200 μM $[Ca^{2+}]_o$, the neurons did maintain a fixed phase shift between each other, demonstrating a constant firing order within a global cycle. A reliable measure of network synchronization is the correlation time lag (*Materials and Methods* and *SI Materials and Methods*, *Analysis*), which is an indicator of the mean phase shifts between the different oscillators. As Fig. 3 *C* and *D* shows, there was a strong decrease in this measure, going from 1.5 s at 100 μM down to 0.015 s at 500 μM $[Ca^{2+}]_o$, corresponding to a similar decrease in the mean phase shifts. Zero-lag occurred at 500 μM, as manifested by synchronized periodic network bursts. Note that the peak in

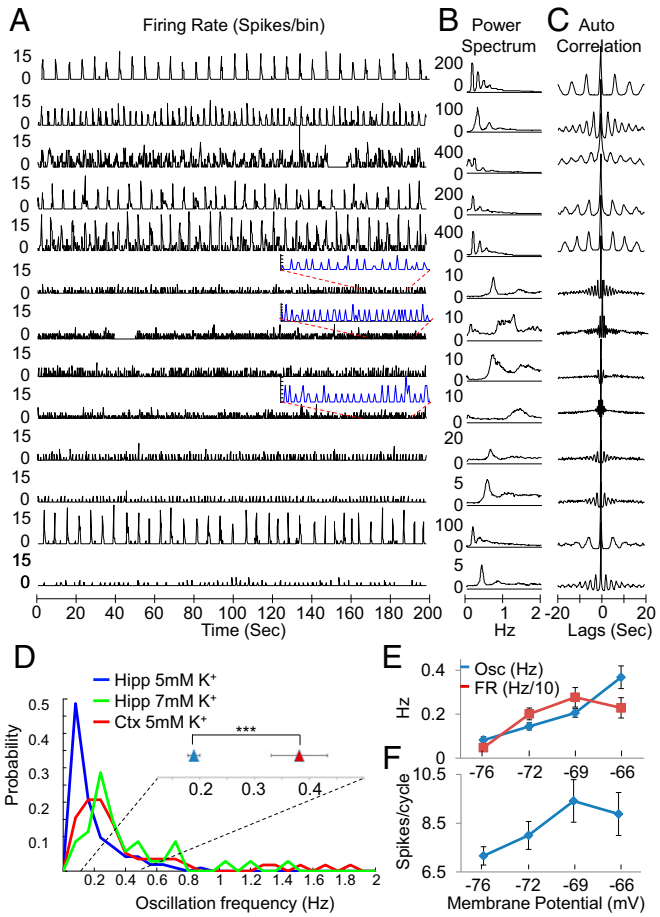

Fig. 2. Oscillatory firing of disconnected neurons in zero-calcium medium. (*A*) Example of firing rate traces for 12 of about 40 neurons from one culture. (*Insets*) Oscillations where the oscillation rate is high but the firing rate is low (typically one to three spikes per oscillation) are emphasized. (*B* and *C*) Power spectrum and autocorrelation of the traces shown in *A* capture the robust and stable oscillatory behavior of the single neurons. (*D*) Probability distribution function of the oscillation frequency for hippocampus under 5 mM $[K^+]_o$ (blue, $n = 216$ electrodes from eight cultures) and 7 mM $[K^+]_o$ (green, $n = 59$ electrodes from three cultures) and for cortical cells under 5 mM $[K^+]_o$ (red, $n = 60$ electrodes from four cultures). (*Inset*) Comparison of the average of the distribution for hippocampus vs. cortex (***$P < 0.001$). (*E*) Average oscillation frequency (Osc; blue) and firing rate (FR; red) of the single neurons increase significantly (ANOVA: $P < 0.001$; $P < 0.0001$, respectively) as a function of potassium concentration (shown are 1, 3, 5, and 7 mM $[K^+]_o$ with corresponding $n = 58$, $n = 61$, $n = 62$, and $n = 59$ electrodes from three cultures). The *x* axis is in units of the membrane rest potential. Note that firing rate units are scaled in hertz/10. (*F*) As in *E* for the average number of spikes per oscillation.

Fig. 3*B* is shown for the correlation of a single electrode, typically the first to fire, with all of the rest of the electrodes.

Fig. 3 points to a two-stage synchronization process. The first stage is an adjustment to one frequency that occurs already at 100 μM. The second stage is full synchronization, with very small or zero time lag and fast recruitment times (*SI Materials and Methods*, *Analysis*), which arises at 500 μM. Interestingly, the mean single neuron oscillation frequency at 0 mM $[Ca^{2+}]_o$ and the mean network burst frequency at 1 mM $[Ca^{2+}]_o$ coincide, as shown in Fig. 3*F* ($n = 6$ cultures).

As mentioned above, there are two mechanisms of calcium-triggered neurotransmitter release at the presynaptic sites. Barium is known to facilitate only the slow-asynchronous release (13, 22). To investigate the relative involvement of the slow-asynchronous

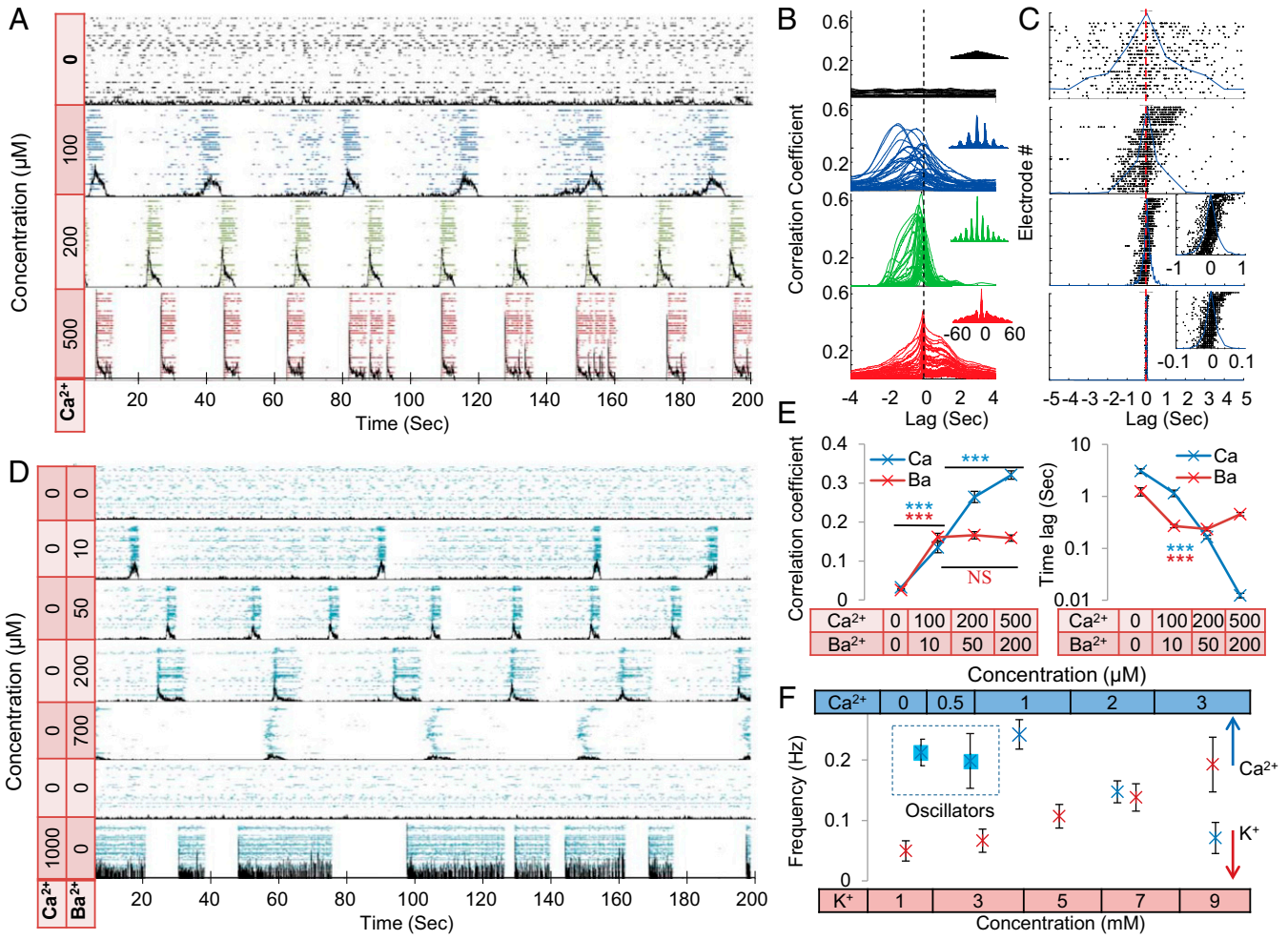

Fig. 3. Transition from independently oscillating single neurons into synchronized network bursts. (*A*) Raster of single neuron activity for 42 electrodes in a sample culture under 5 mM K^+ and increasing $[Ca^{2+}]_o$. Black traces are the sum over spikes in all of the electrodes per 20-ms bins, representing total network activity. (*B*) Sample of cross-correlation function for one electrode with all of the other electrodes in the culture shown in *A*, taken over 25 min. (*Insets*) Zoom-out view of each cross-correlation function, emphasizing the long-term coherence of the oscillations, and therefore the stability of the synchrony. (*C*) Lags at which the peak of the correlation functions (like the examples shown in *B*) were attained for all of the electrodes in *A*. The blue trace is the normalized histogram of the electrodes per lag in 200-ms bins. (*Insets*) Lags and histograms in 20-ms bins. Electrodes have been ordered along the *y* axis by the sum over the lags in the *x* axis (this order is different from the order in *A*), and the general monotonic tilt of the data shows that the order between electrode firing is maintained. (*D*) Raster of single neuron activity for 41 electrodes in a sample culture under an increasing concentration of barium. In the lowest two panels, the barium was washed away, and in the lowest panel, 1 mM $[Ca^{2+}]_o$ was added. Black traces are the sum over spikes in all of the electrodes per 20-ms bins, representing total network activity. (*E*) Average over all electrodes of the peak values of the cross-correlation coefficients (*Left*) and the corresponding lags themselves (*Right*), under increasing $[Ca^{2+}]_o$ (blue) and barium (red). This lag gives a characteristic of the synchrony (*Materials and Methods* and *SI Materials and Methods, Analysis*). *P* values were computed using single-factor ANOVA (***$P < 0.001$). Interactions were significant for all $[Ca^{2+}]_o$ values but only for 0 mM barium (post hoc analysis). (*F*) Change in frequency as a function of $[Ca^{2+}]_o$ (blue) and of $[K^+]_o$ (red). The lower two concentrations of $[Ca^{2+}]_o$ (dashed rectangle) have independently oscillating neurons, and the value given is the average over their frequencies; all other frequencies are for the synchronized network bursts. No difference (*t* test: $P = 0.423$) was found between the average oscillation frequency (at 0 mM) and the network burst frequency (at 1 mM). Both calcium and potassium effects on network burst frequency were significant (ANOVA: ***$P < 0.001$; NS, not significant).

(scale of seconds) release, we introduced a gradual increase of $[Ba^{2+}]_o$ while keeping $[Ca^{2+}]_o$ at 0 mM (Fig. 3*D*).

Similar to calcium, adding barium gradually increased the tendency of the whole population to oscillate at one frequency. However, the added barium did not cause the zero-lag synchrony and network bursts that characterize the presence of calcium. Washing the Ba^{2+} retrieved the intrinsic single neuron behavior, whereas further addition of Ca^{2+} brought back the fast, synchronized network bursts, although they were longer than the standard.

Intrinsic Excitability Mechanism Is Mediated by a Sodium Leak Current $I_{Na}P$. Intrinsic firing mechanisms of individual neurons have been suggested to rely on leak currents, which affect neuronal excitability and support oscillatory behavior (14, 23). This leak current often involves the persistent noninactivating sodium current $I_{Na}P$. The relevance of $I_{Na}P$ can be tested by its antagonist riluzole (24, 25). As shown in Fig. 4*A*, the addition of 1 μM riluzole immediately and dramatically reduced all activity of the neurons. At 0 mM $[Ca^{2+}]_o$ and 1 μM riluzole, over 70% of the active neurons ceased their activity completely, whereas the mean firing rate decreased by about 90% in the remaining 30%.

Upon addition of 1 mM Ca^{2+}, practically all of the neurons regained synchronous activity, but the burst rate remained extremely low (Fig. 4*B*), with quiescent periods on the order of minutes between bursts. Most suggestive is that the bursts that did occur with riluzole exhibited zero-lag synchrony, which is characteristics of regular connected networks at 1 mM $[Ca^{2+}]_o$. Washout of the riluzole brought about almost full recovery of the

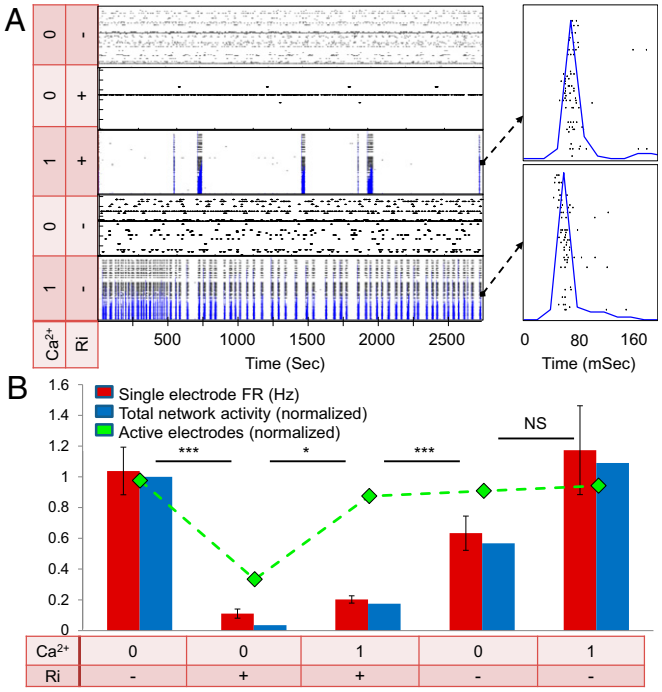

Fig. 4. Intrinsic excitability mechanism is mediated by a persistent sodium leak current. (*A*) Raster of single neuron activity for 30 electrodes in a sample culture under different conditions of calcium and riluzole. Blue traces are the sum over spikes in all of the electrodes per 20-ms bins, representing total network activity. The lowest two panels are after washing out of the riluzole. (*Right*) Blow-up view of a single network burst in the 1 mM $[Ca^{2+}]_o$ conditions, either with riluzole (*Top*) or after washing it out (*Bottom*). (*B*) Effect of riluzole on single electrode and network activity. As a baseline for comparison and normalization, 0 mM $[Ca^{2+}]_o$ and no riluzole (Ri) are used. Single electrode firing rates (red bars), relative number of active electrodes (green curve), and network activity (blue bars) are greatly reduced by riluzole application at 0 mM $[Ca^{2+}]_o$ ($n = 57$; t test: $P < 0.0001$). The network activity was calculated as the total number of recorded spikes divided by time (in seconds) and is presented as the change relative to the condition before riluzole. Adding 1 mM calcium results in only a small recovery in firing rates (t test: $^*P < 0.05$; $^{***}P < 0.001$) and total activity, but the number of active electrodes is concurrently almost completely recovered in these conditions. The effect of riluzole is most pronounced in the total network activity (blue bars), which actually equals the value of the single electrode activity (red bars) multiplied by the value of the number of active electrodes (green curve).

intrinsic neuronal firing at 0 mM $[Ca^{2+}]_o$ and of the network activity at 1 mM $[Ca^{2+}]_o$.

Discussion

We have shown that under sufficient excitability conditions, about 60% of dissociated, disconnected hippocampal or cortical neurons will oscillate. This intrinsic excitability is supported by the sodium leak current $I_{Na}P$, and is strongly affected by calcium levels. Upon a gradual increase in connectivity, the entrainment of these intrinsic oscillations through decreasing phase shifts was found to underlie the emergence of synchronized and periodic network bursts. Our use of synaptic blockers elucidated the involvement of neurotransmission in coupling the individual neurons, but coupling mechanisms such as gap junctions (26, 27) and glial cells should also be considered (*SI Discussion*).

The importance of elevated calcium concentrations is twofold, enabling network connectivity by increasing the synaptic release while concurrently reducing the single neuron excitability. The effect of excitability is dominant in allowing the intrinsic oscillations and in determining their frequency. A minimal excitability is also required for the activation of the sodium leak current $I_{Na}P$. The increase in excitability obtained by depolarizing the resting membrane potential via the potassium concentration leads to an increase in the single neuron oscillation frequencies. Addition of magnesium, a divalent ion-like calcium, decreased the excitability without affecting the connectivity.

The effect of calcium on excitability also explains why disconnecting the network via synaptic blockers at elevated calcium levels stops practically all activity. Our picture of the bursting network activity at elevated calcium is based on the idea that without blockers, a background of spontaneous synaptic activity exists and makes the neurons slightly more excitable. We have shown previously that under these conditions of strong connectivity, firing of a small fraction of the neurons, presumably those neurons that are more sensitive to inputs and lead the activity, suffices to ignite the rest of the network (28–30). An additional effect of increased network synchronization with elevated $[Ca^{2+}]_o$ was recently reported in cortical slices (31), but through differential sensitivity of excitatory and inhibitory synapses to calcium.

The contribution of calcium in enabling connectivity and the build-up of synchronization is also dual, this time because of the two main mechanisms for vesicle release. The interplay between calcium-dependent fast-synchronous and slow-asynchronous neurotransmitter release is central to understanding the dynamics in this system. The slow-release mechanism is sufficient to adjust the frequencies of the individual oscillators into a unified oscillation frequency, but not to synchronize the oscillators, which requires the addition of fast release. This effect is also seen in conditions of no calcium but with barium, which enables only the slow release. Zero-lag synchronization occurs at elevated calcium concentrations, presumably when the fast-release mechanism is activated as well, making the coupling stronger. This interplay is explained by different sensitivities of the two mechanisms to intracellular calcium concentrations (32).

Within theoretical models for self-entrainment of independent oscillators (20, 21, 33, 34), the coupling strength determines the synchronization process. In our system, the connectivity, or coupling, is controlled by the calcium concentration. The original model by Kuramoto (20) makes a clear prediction that the network will oscillate at a fixed frequency that equals the average of the frequencies of the single oscillators. For more complex pulse-coupled models, the network burst frequency may be a complex function of the coupling strength (20, 34–36). Our measurements indicate that at least at one point (5 mM $[K^+]_o$ and 1 mM $[Ca^{2+}]_o$), there is a correspondence between the burst frequency and the average of single neuron frequencies, much like the model prediction of Kuramoto (20). However, from Fig. 3, it can be seen that increasing the coupling strength also decreases the burst frequency, which is different from the simple scenario of Kuramoto (20). Interestingly, Hansel et al. (35) showed that the frequency tends to a steady value as the coupling increases to unity. This result may indicate that at 1 mM $[Ca^{2+}]_o$, the system has reached a strong coupling limit.

Another deviation of our data from the predictions of theoretical models can be seen in the comparison between the stability of the single neuron oscillations and those oscillations of the network bursts. Theoretically, the coupling of the oscillators should lead to an improvement of the precision of the oscillators (37). However, we have seen clearly that the single neuron oscillations are, in fact, 30% more precise than the network bursts, as measured by the IBI distribution functions and their CV.

The deviations may be because these models often make assumptions that are not borne out experimentally, for example, that the coupling is uniform, that there is no inhibition, and that the distribution function of the frequencies is symmetrical around the mean. The coupling in our system is more complex because it is composed of two components, the slow-vesicle release and the fast-vesicle release. Furthermore, we have shown that neuronal excitability is important in determining the frequency of oscillations and

the extent of network activation, a factor usually ignored in models of synchronizing oscillators. For example, the excitability must cross a threshold to enable the oscillatory behavior. Another difference from the models is that a small subpopulation of active neurons suffices to ignite the rest of the network (29).

An interesting point is that in our experimental setup, both single neuron and network oscillation frequencies are robust and stable for hours. However, in a medium with horse serum, a totally different behavior emerges (Fig. S5). The same network architecture can thus switch between different modes of dynamics by only changing the fluid environment, with no need for an associated change in the hardwiring of synaptic connectivity.

In summary, cultured neurons comprise a network of coupled intrinsic oscillators that may be described by theoretical models for self-emergent synchronization. In this scenario, the slow, calcium-dependent, asynchronous release is a weak coupling that suffices to entrain the frequencies of the oscillators, whereas the fast, calcium-dependent, synchronous release is required to attain zero-lag synchrony. Once coupling is established in the network, the oscillators converge onto one frequency, which is close to the mean distribution of their natural frequencies. Thus, the intrinsic oscillations characteristic of the majority of neurons, and the resultant network periodicity in the shape of rhythmic bursts, may play an important role in defining the dynamical states in many neuronal processes (38).

Materials and Methods

Rat hippocampal neurons from 19-d-old embryos were used (39). All procedures were approved by the Weizmann Institute's Animal Care and Use Committee. Measurements were typically carried out on 14–17 DIV (one measurement was on 19 DIV) in a chamber placed on a plate that was temperature-controlled by circulation of water at 38 °C. MEAs of 60 electrodes of with a diameter of 30 μm and a spacing of 200 μM (MultiChannelSystems) were used for recording (Fig. S9). The electrical signals were amplified 1,200-fold and sampled at 13 kHz, using a general purpose digital-to-analog converter. Data were acquired and processed using MATLAB (The MathWorks). Electrodes were deemed active and retained for further analysis if the mean firing rate during the measurement was above 0.01 Hz. Both single neuron oscillations and periodic network bursts were identified by the FFT. Synchrony was defined by the cross-correlation of all of the electrodes with each other. The time lag at which the averaged cross-correlation has a peak was extracted for each pair of electrodes. The average over these time lags serves as a quantitative measure of network synchrony. Zero-lag (maximal) synchrony was defined to occur if this average time lag drops to less than 20 ms (Fig. 3*C*, *Bottom*). Recruitment time was defined as the duration between the first spike in the burst and when 80% of the participating neurons fired their first spike. To demonstrate that the phase shift between the neurons is fixed, and thus the order of firing of the neurons within the burst is fixed, the electrodes have been ordered in Fig. 3*C* according to the mean lag with all of the other electrodes. Barium was added in the form of $BaCl_2$ at concentrations varying from 2 μM to 3 mM. Riluzole (R116-25MG; Sigma) was administered at 0.3–10 μM to block the persistent sodium current I_{NaP}. Details are provided in *SI Materials and Methods*.

ACKNOWLEDGMENTS. We thank S. Bottani, D. Freche, I. Lampl, and S. Stern for discussions and advice. This work was supported by the Minerva Foundation and the Israel Science Foundation (ISF 12/1415).

1. Chorev E, Yarom Y, Lampl I (2007) Rhythmic episodes of subthreshold membrane potential oscillations in the rat inferior olive nuclei in vivo. *J Neurosci* 27(19):5043–5052.
2. Llinás RR (1988) The intrinsic electrophysiological properties of mammalian neurons: Insights into central nervous system function. *Science* 242(4886):1654–1664.
3. Buzsáki G (2006) *Rhythms of the Brain* (Oxford Univ Press, New York).
4. Turrigiano G (2011) Too many cooks? Intrinsic and synaptic homeostatic mechanisms in cortical circuit refinement. *Annu Rev Neurosci* 34:89–103.
5. Blankenship AG, Feller MB (2010) Mechanisms underlying spontaneous patterned activity in developing neural circuits. *Nat Rev Neurosci* 11(1):18–29.
6. Takahashi N, Sasaki T, Matsumoto W, Matsuki N, Ikegaya Y (2010) Circuit topology for synchronizing neurons in spontaneously active networks. *Proc Natl Acad Sci USA* 107(22):10244–10249.
7. Brocard F, et al. (2013) Activity-dependent changes in extracellular Ca2+ and K+ reveal pacemakers in the spinal locomotor-related network. *Neuron* 77(6):1047–1054.
8. Markram H, et al. (2004) Interneurons of the neocortical inhibitory system. *Nat Rev Neurosci* 5(10):793–807.
9. Fröhlich F, Bazhenov M, Timofeev I, Steriade M, Sejnowski TJ (2006) Slow state transitions of sustained neural oscillations by activity-dependent modulation of intrinsic excitability. *J Neurosci* 26(23):6153–6162.
10. Izhikevich EM (2000) Neural excitability, spiking and bursting. *Int J Bifurcat Chaos* 10(6):1171–1266.
11. Cohen I, Miles R (2000) Contributions of intrinsic and synaptic activities to the generation of neuronal discharges in in vitro hippocampus. *J Physiol* 524(Pt 2):485–502.
12. Konnerth A, Heinemann U, Yaari Y (1986) Nonsynaptic epileptogenesis in the mammalian hippocampus in vitro. I. Development of seizurelike activity in low extracellular calcium. *J Neurophysiol* 56(2):409–423.
13. Bacaj T, et al. (2013) Synaptotagmin-1 and synaptotagmin-7 trigger synchronous and asynchronous phases of neurotransmitter release. *Neuron* 80(4):947–959.
14. Xiong Z, Lu W, MacDonald JF (1997) Extracellular calcium sensed by a novel cation channel in hippocampal neurons. *Proc Natl Acad Sci USA* 94(13):7012–7017.
15. Lu B, et al. (2010) Extracellular calcium controls background current and neuronal excitability via an UNC79-UNC80-NALCN cation channel complex. *Neuron* 68(3):488–499.
16. Eytan D, Marom S (2006) Dynamics and effective topology underlying synchronization in networks of cortical neurons. *J Neurosci* 26(33):8465–8476.
17. Borst JG, Sakmann B (1996) Calcium influx and transmitter release in a fast CNS synapse. *Nature* 383(6599):431–434.
18. Del Castillo J, Katz B (1954) Quantal components of the end-plate potential. *J Physiol* 124(3):560–573.
19. Robinson HP, et al. (1993) Periodic synchronized bursting and intracellular calcium transients elicited by low magnesium in cultured cortical neurons. *J Neurophysiol* 70(4):1606–1616.
20. Kuramoto Y (1975) Self-entrainment of a population of coupled non-linear oscillators. *International Symposium on Mathematical Problems in Theoretical Physics* (Springer, Berlin), pp 420–422.
21. Strogatz SH (2000) From Kuramoto to Crawford: Exploring the onset of synchronization in populations of coupled oscillators. *Physica D* 143(1):1–20.
22. Bhalla A, Tucker WC, Chapman ER (2005) Synaptotagmin isoforms couple distinct ranges of Ca2+, Ba2+, and Sr2+ concentration to SNARE-mediated membrane fusion. *Mol Biol Cell* 16(10):4755–4764.
23. Tazerart S, Vinay L, Brocard F (2008) The persistent sodium current generates pacemaker activities in the central pattern generator for locomotion and regulates the locomotor rhythm. *J Neurosci* 28(34):8577–8589.
24. Koizumi H, Smith JC (2008) Persistent Na+ and K+-dominated leak currents contribute to respiratory rhythm generation in the pre-Bötzinger complex in vitro. *J Neurosci* 28(7):1773–1785.
25. Le Bon-Jego M, Yuste R (2007) Persistently active, pacemaker-like neurons in neocortex. *Front Neurosci* 1(1):123–129.
26. Draguhn A, Traub RD, Schmitz D, Jefferys JG (1998) Electrical coupling underlies high-frequency oscillations in the hippocampus in vitro. *Nature* 394(6689):189–192.
27. Rouach N, Segal M, Koulakoff A, Giaume C, Avignone E (2003) Carbenoxolone blockade of neuronal network activity in culture is not mediated by an action on gap junctions. *J Physiol* 553(Pt 3):729–745.
28. Eckmann JP, Jacobi S, Marom S, Moses E, Zbinden C (2008) Leader neurons in population bursts of 2D living neural networks. *New J Phys* 10(1):015011.
29. Soriano J, Rodríguez Martínez M, Tlusty T, Moses E (2008) Development of input connections in neural cultures. *Proc Natl Acad Sci USA* 105(37):13758–13763.
30. Orlandi JG, Soriano J, Alvarez-Lacalle E, Teller S, Casademunt J (2013) Noise focusing and the emergence of coherent activity in neuronal cultures. *Nat Phys* 9(9):582–590.
31. Markram H, et al. (2015) Reconstruction and Simulation of Neocortical Microcircuitry. *Cell* 163(2):456–492.
32. Pang ZP, Südhof TC (2010) Cell biology of Ca2+-triggered exocytosis. *Curr Opin Cell Biol* 22(4):496–505.
33. Mirollo RE, Strogatz SH (1990) Synchronization of pulse-coupled biological oscillators. *SIAM J Appl Math* 50(6):1645–1662.
34. Ermentrout GB (1985) Synchronization in a pool of mutually coupled oscillators with random frequencies. *J Math Biol* 22(1):1–9.
35. Hansel D, Mato G, Meunier C (1993) Phase dynamics for weakly coupled Hodgkin-Huxley neurons. *Europhys Lett* 23(5):367–372.
36. Ermentrout GB, Kopell N (1991) Multiple pulse interactions and averaging in systems of coupled neural oscillators. *J Math Biol* 29(3):195–217.
37. Kori H, Kawamura Y, Masuda N (2012) Structure of cell networks critically determines oscillation regularity. *J Theor Biol* 297:61–72.
38. Llinás RR (2013) The olivo-cerebellar system: A key to understanding the functional significance of intrinsic oscillatory brain properties. *Front Neural Circuits* 7:96.
39. Segal M, Manor D (1992) Confocal microscopic imaging of [Ca2+]i in cultured rat hippocampal neurons following exposure to N-methyl-D-aspartate. *J Physiol* 448: 655–676.